

Boundary renormalisation group flows of the supersymmetric Lee–Yang model and its extensions

Márton Kormos*

*Institute for Theoretical Physics, Eötvös University,
1117 Budapest, Pázmány Péter sétány 1/A, Hungary*

May 2, 2007

Abstract

In this paper we examine the supersymmetric Lee–Yang model in the presence of boundaries. We determine the reflection factors for the Neveu–Schwarz type boundary conditions from the reduction of the supersymmetric sine–Gordon model and check them by using Boundary Truncated Conformal Space Approach in the massless case. We explore the boundary renormalisation groups flows using boundary TBA and TCSA.

*kormos@general.elte.hu

1 Introduction

Boundary conformal field theories attracted much interest recently, due to their applications in describing D-branes in string theory [1, 2] and their relevance in condensed matter physics, e. g. in the Kondo problem [3].

Several papers appeared in the literature that deal with the consistent boundary conditions and reflection factors [4, 5, 6, 7, 8, 9], the boundary perturbations and the corresponding renormalisation flows [10, 11, 12, 13] of two-dimensional supersymmetric field theories.

One of the simplest supersymmetric theory is the supersymmetric Lee–Yang (SLY) model and in this paper we study this model in the presence of boundaries. In a paper [12] Ahn and Nepomechie proposed reflection factors for the superconformal boundary conditions and determined a boundary flow using Boundary Thermodynamic Bethe Ansatz (BTBA). Here we argue that both their reflection factor and one of their TBA formulae are mistaken. We propose different reflection factors which we check using Boundary Truncated Conformal Space Approach (BTCSA). We also predict a different boundary flow using BTBA and we compare the fixed points and the change of the boundary entropy again with our BTCSA results.

The paper is organized as follows. In section 2 we summarize some basic facts about the SLY model. In section 3 we determine the reflection factors by applying a “folding” trick to the supersymmetric sine–Gordon reflection factors. In section 4 some details of the BTCSA are explained briefly and after calculating the massless reflection factors the predicted energy levels and phase shifts are compared to the BTCSA results. In section 5 we write down the BTBA equations and calculate the variation of the g -function along the boundary flow. In section 6 this is compared to the BTCSA result for the fixed points and the g -function. Finally, in section 7 we extend our study of the flows to the models $SM(2, 4n + 4)$ which are the generalisations of the SLY model.

2 The supersymmetric Lee–Yang model

The supersymmetric Lee–Yang model or the superconformal minimal model $SM(2,8)$ is a non-unitary conformal field theory with central charge $c = -\frac{21}{4}$. The super Kac-table with the highest weights of the primary fields is

0	$-\frac{3}{32}$	$-\frac{1}{4}$	$-\frac{7}{32}$	$-\frac{1}{4}$	$-\frac{3}{32}$	0
---	-----------------	----------------	-----------------	----------------	-----------------	---

The algebra of superconformal transformations in the plane are generated by two fields, $T(z)$ and $G(z)$ whose mode expansions read

$$T(z) = \sum_n L_n z^{-n-2}, \quad (2.1a)$$

$$G(z) = \sum_r G_r z^{-r-3/2}. \quad (2.1b)$$

The $N = 1$ supersymmetric extension of the Virasoro algebra is defined by the following (anti)commutation relations:

$$[L_n, L_m] = (n - m)L_{n+m} + \frac{c}{12}n(n^2 - 1)\delta_{n,-m}, \quad (2.2a)$$

$$\{G_r, G_s\} = 2L_{r+s} + \frac{c}{3}(r^2 - 1/4)\delta_{r,-s}, \quad (2.2b)$$

$$[L_n, G_r] = \left(\frac{n}{2} - r\right)G_{n+r}. \quad (2.2c)$$

Here n, m denote integers, while depending on the boundary conditions for $G(z)$ the indices r, s can take half-integer (Neveu–Schwarz sector) or integer (Ramond sector) values.

The highest weight representations of the algebra are defined by highest weight states $|\Delta\rangle$ satisfying

$$L_n|\Delta\rangle = 0 \quad n > 0, \quad (2.3a)$$

$$L_0|\Delta\rangle = \Delta, \quad (2.3b)$$

$$G_r|\Delta\rangle = 0 \quad r > 0. \quad (2.3c)$$

The Verma module is generated by operators having a nonpositive index. The vectors

$$L_{n_1} \dots L_{n_k} G_{r_1} \dots G_{r_l} |\Delta\rangle, \quad n_1 \leq \dots \leq n_k < 0, \quad r_1 < \dots < r_l \leq 0 \quad (2.4)$$

constitute a basis for the Verma module. Note that the inequalities for the r_i -s are strict since $G_r^2 = L_{2r} - \frac{c}{12}\delta_{r,0}$ by equation (2.2b).

In this paper we consider the so-called spin model which can be obtained by the projection onto the states with even fermion parity of the Hilbert space.

One can consider this superminimal model on a strip of width R with nontrivial boundary conditions at the edges of the strip. In the Ramond sector the superconformal boundary conditions are in one-to-one correspondence with the highest weight representations so they can be indexed by the same label set (the Kac indices), whereas in the Neveu–Schwarz sector there are two boundary conditions for each entry of the Kac table, the NS and the \bar{NS} boundary conditions [4].

This model can also be defined as the minimal model $M(3,8)$ with Kac table

0	-7/32	-1/4	-3/32	1/4	25/32	3/2
3/2	25/32	1/4	-3/32	-1/4	-7/32	0

Suitable combinations of the Virasoro representations constitute irreducible representations of the superconformal algebra:

$$\left(0\right)_{\text{SVir}} \longleftrightarrow \left(0\right)_{\text{Vir}} \oplus \left(\frac{3}{2}\right)_{\text{Vir}} \quad (2.5a)$$

$$\left(-\frac{1}{4}\right)_{\text{SVir}} \longleftrightarrow \left(-\frac{1}{4}\right)_{\text{Vir}} \oplus \left(\frac{1}{4}\right)_{\text{Vir}} \quad (2.5b)$$

$$\left(-\frac{7}{32}\right)_{\text{SVir}} \longleftrightarrow \left(-\frac{7}{32}\right)_{\text{Vir}} \oplus \left(\frac{25}{32}\right)_{\text{Vir}}. \quad (2.5c)$$

$$\left(-\frac{3}{32}\right)_{\text{SVir}} \longleftrightarrow \left(-\frac{3}{32}\right)_{\text{Vir}}. \quad (2.5d)$$

Since the superprimary fields are also Virasoro primary fields and the g -factors are the same for the NS and $\widetilde{\text{NS}}$ boundaries, the g -factors of the various conformal boundary conditions can be calculated in the Virasoro picture. The matrix elements of the S modular transformation are

$$S_{(r,s),(r',s')} = 2\sqrt{\frac{2}{pq}}(-1)^{rs'+r's+1} \sin\left(rr'\frac{q}{p}\pi\right) \sin\left(ss'\frac{p}{q}\pi\right) \quad (2.6)$$

and according to [14] the g -factors are given by

$$g_{(1,s)} = \frac{S_{\Omega,(1,s)}}{\sqrt{|S_{\Omega,0}|}} \quad (2.7)$$

where 0 denotes the conformal vacuum and Ω denotes the state of lowest conformal weight. In our case $0 = (1, 1)$ and $\Omega = (1, 3)$, so

$$g_{(1,s)} = \frac{(-1)^s \sin \frac{9\pi}{8}s}{\sqrt{2} \sqrt{\sin \frac{\pi}{8}}}. \quad (2.8)$$

If we choose the $\beta = (1, 1)$ boundary condition at one of the edges and $\alpha = (1, s)$ at the other one, the partition function on a cylinder of circumference L and length R will be

$$\begin{aligned} \mathcal{Z}(R, L) = \text{tr}_{\widetilde{\text{NS}}} \frac{1 + (-1)^F}{2} e^{-LH_{(1,1),(1,s)}} + \text{tr}_{\text{R}} \frac{1 + (-1)^F}{2} e^{-LH_{(1,1),(1,s)}} = \\ \text{tr}_{(1,s)} \frac{1 \pm (-1)^F}{2} e^{-\pi \frac{L}{R}(L_0 - c/24)}, \quad (2.9) \end{aligned}$$

where the sign is “+” if both boundaries are of NS or $\widetilde{\text{NS}}$ type and “−” if they are different (see [4, 13] for details). Thus the Hilbert space consists of the *bosonic levels* of the corresponding superconformal Verma module *if the boundary conditions are both of NS or $\widetilde{\text{NS}}$ type* and of the *fermionic levels* of this module *if they are different*. For a bosonic primary field the bosonic levels are the integer levels and for a fermionic primary field they are the half-integer levels.

We consider the boundary perturbation of this model defined by the action:

$$\mathcal{A} = \mathcal{A}_{\text{SM}(2,8)} + h \int_{-\infty}^{\infty} dt (\hat{G}_{-1/2}\phi_{1,3})(0, t). \quad (2.10)$$

where $(\hat{G}_{-1/2}\phi)$ is the field appearing in the operator product expansion of $G(z)$ and ϕ :

$$G(z)\phi(w) = \frac{(\hat{G}_{-1/2}\phi)(w)}{z-w} + \dots \quad (2.11)$$

This operator can live on the $(1, s)$ boundary since the fusion coefficient $N_{(1,3),(1,s)}^{(1,s)}$ is non-zero. This boundary perturbation is relevant, since the conformal dimension of the perturbing operator is $1/4 < 1$. Since there is no perturbation in the bulk, the theory remains massless along the flow. The perturbation preserves supersymmetry so the boundary renormalisation group flows will take place in the space of possible supersymmetric boundary conditions, in which the fixed points are the superconformal ones. This perturbation is also integrable [15].

3 The reflection factor

We obtain the S-matrix and the reflection factor of the supersymmetric Lee–Yang model by considering it as a reduction of the supersymmetric sine–Gordon (SSG) model. The original idea is of Smirnov [16] and it was first applied in supersymmetric context for bulk S-matrices in [17]. The SSG S-matrix was also derived in [17], the formulae are collected in appendix A.

If $\lambda > 2$ in the sine–Gordon model the pole in the S-matrix describing the scattering of the first breather on itself corresponds to the second breather as a bound state. For $\lambda < 2$ only the first breather is in the spectrum and the pole is explained by the Coleman–Thun mechanism [18] which requires the presence of solitons in the theory. However, at the particular value of the coupling constant $\lambda = \frac{3}{2}$ the masses and the S-matrices for the first and the would-be second breathers become equal: $m_1 = m_2$ and $S_{\text{SSG}}^{1,1} = S_{\text{SSG}}^{1,2} = S_{\text{SSG}}^{2,2}$, so the pole can be explained by the self fusion of the only breather and the solitons can be projected out consistently from the theory [17]. Thus the SSG model is reduced to the supersymmetric scaling Lee–Yang model containing only one superdoublet. The S-matrix simplifies to

$$S_{\text{SLY}}(\theta) = S_{\text{LY}}(\theta)S_{\text{SUSY}}(\theta) \quad (3.1)$$

where

$$S_{\text{LY}}(\theta) = \frac{\sinh(\theta) + i \sin(\frac{2\pi}{3})}{\sinh(\theta) - i \sin(\frac{2\pi}{3})} \quad (3.2)$$

and

$$S_{\text{SUSY}}(\theta) = \tilde{Z}(\theta) \times \begin{pmatrix} 1 + 2i \frac{\sin(\frac{\pi}{3})}{\sinh(\theta)} & 0 & 0 & \frac{\sin(\frac{\pi}{3})}{\cosh(\frac{\theta}{2})} \\ 0 & 1 & i \frac{\sin(\frac{\pi}{3})}{\sinh(\frac{\theta}{2})} & 0 \\ 0 & i \frac{\sin(\frac{\pi}{3})}{\sinh(\frac{\theta}{2})} & 1 & 0 \\ \frac{\sin(\frac{\pi}{3})}{\cosh(\frac{\theta}{2})} & 0 & 0 & -1 + 2i \frac{\sin(\frac{\pi}{3})}{\sinh(\theta)} \end{pmatrix}, \quad (3.3)$$

$$\tilde{Z}(\theta) = \frac{\sinh(\frac{\theta}{2})}{\sinh(\frac{\theta}{2}) + i \sin(\frac{\pi}{3})} \exp \left\{ \int_0^\infty \frac{dt \sinh(\frac{t}{3}) \sinh(\frac{2t}{3})}{t \cosh^2(\frac{t}{2}) \cosh(t)} \sinh(\frac{it\theta}{\pi}) \right\}. \quad (3.4)$$

This is the S-matrix used also by Ahn and Nepomechie in [12]. For later convenience we introduce the notation

$$Z(\theta) = S_{\text{LY}}(\theta) \tilde{Z}(\theta). \quad (3.5)$$

It is easy to check that this S-matrix satisfies the appropriate unitarity and crossing relations and that the Yang–Baxter equations are also satisfied.

3.1 The “folding”

We have seen that at the particular coupling $\lambda = \frac{3}{2}$ the bulk SSG model reduces to the SLY model. For this reduction to be consistent also in the boundary case it is necessary that at this point the reflection factors for the 1st and the would-be 2nd breather be equal. This requirement gives functional relations between the two SSG boundary parameters, η and ϑ (first considered in [8]).

The reflection factors of the boundary SSG model can be found in appendix B. In the $BSSG^+$ case the supersymmetric factor $R_{\text{SUSY}}(\theta)$ (see B.8) does not contain the boundary parameters and the only way it depends on the species of the breather is through the parameter ρ which at this special coupling is $\rho_k = \pi - k\frac{2\pi}{3}$. From $\rho_1 = -\rho_2 = \frac{\pi}{3}$ it is obvious that $\mathcal{A}_\pm(\theta)$ are automatically the same for $k = 1, 2$.

Now we turn to the scalar part, i. e. to the SG reflection factors. It turns out that $R^{(1)}(\theta) = R^{(2)}(\theta)$ if

$$\eta = i\vartheta + \frac{2k+1}{2}\pi, \quad k \in \mathbb{Z}. \quad (3.6)$$

If $k = 1$, i. e. $\eta = i\vartheta + \frac{3\pi}{2}$ then $R^{(1)} = R^{(2)} = R_0$ where

$$R_0(\theta) = \left(\frac{1}{2}\right) \left(\frac{3}{2}\right) \left(\frac{4}{2}\right)^{-1}, \quad (3.7)$$

where we introduced the notation

$$(x) = \frac{\sin(\frac{\theta}{2i} + x\frac{\pi}{6})}{\sin(\frac{\theta}{2i} - x\frac{\pi}{6})}.$$

If $k = 1$, i. e. $\eta = i\vartheta + \frac{\pi}{2}$ then $R^{(1)} = R^{(2)} = R_I$ with

$$R_I(\theta) = R_0(\theta) \left(\frac{1+b}{2} \right) \left(\frac{1-b}{2} \right)^{-1} \left(\frac{5-b}{2} \right) \left(\frac{5+b}{2} \right)^{-1} = R_0(\theta) \left(S_{\text{LY}} \left(\theta + i \frac{b+3}{6} \pi \right) S_{\text{LY}} \left(\theta - i \frac{b+3}{6} \pi \right) \right)^{-1}, \quad (3.8)$$

where we introduced the parameter $b = \frac{4i}{\pi}\vartheta - 2$. $R_0(\theta)$ and $R_I(\theta)$ are the same reflection factors as those given by Dorey et al. (for example in [19]).

Finally, if $k = -1$, i. e. $\eta = i\vartheta - \frac{\pi}{2}$ then $R^{(1)} = R^{(2)} = R_{II}$ where

$$R_{II}(\theta) = R_0(\theta) \left(\frac{b-1}{2} \right) \left(\frac{b+3}{2} \right)^{-1} \left(\frac{b-3}{2} \right) \left(\frac{5+b}{2} \right)^{-1} = R_0(\theta) \left(S_{\text{LY}} \left(\theta + i \frac{b+1}{6} \pi \right) S_{\text{LY}} \left(\theta - i \frac{b+1}{6} \pi \right) \right)^{-1}. \quad (3.9)$$

The other values of k do not lead to new reflection factors. With the redefinition $b \rightarrow b + 4$ the factor $R_{II}(\theta)$ becomes

$$R_{II}(\theta) = R_0(\theta) \left(\frac{b+3}{2} \right) \left(\frac{5-b}{2} \right) \left(\frac{b+1}{2} \right) \left(\frac{3-b}{2} \right) = R_0(\theta) \left(S_{\text{LY}} \left(\theta + i \frac{b+5}{6} \pi \right) S_{\text{LY}} \left(\theta - i \frac{b+5}{6} \pi \right) \right)^{-1}, \quad (3.10)$$

which can be identified as the reflection factor for the excited boundary [19]. Thus R_0 and R_I are the two ground state reflection factors for the two boundary conditions of the Lee–Yang model. They satisfy the boundary unitarity and boundary crossing equations:

$$R(\theta)R(-\theta) = 1, \quad (3.11)$$

$$R\left(\frac{i\pi}{2} - \theta\right) = S_{\text{LY}}(2\theta)R\left(\frac{i\pi}{2} + \theta\right). \quad (3.12)$$

The SLY reflection factors also satisfy the boundary unitarity equation provided $\mathcal{A}_{\pm}(\theta)\mathcal{A}_{\pm}(-\theta) = 1$ and this is indeed true:

$$\mathcal{A}_{\pm}(\theta)\mathcal{A}_{\pm}(-\theta) = 2 \frac{\cos\left(\frac{\theta}{2i} \mp \frac{\pi}{4}\right) \cos\left(-\frac{\theta}{2i} \mp \frac{\pi}{4}\right)}{\cosh(\theta)} = 1. \quad (3.13)$$

The boundary crossing equations are

$$2^{-\frac{2\theta}{i\pi}} R_{\phi}^{\phi} \left(\frac{i\pi}{2} - \theta \right) = S_{\phi\phi}^{\phi\phi}(2\theta) R_{\phi}^{\phi} \left(\frac{i\pi}{2} + \theta \right) + S_{\psi\psi}^{\phi\phi}(2\theta) R_{\psi}^{\psi} \left(\frac{i\pi}{2} + \theta \right), \quad (3.14a)$$

$$2^{-\frac{2\theta}{i\pi}} R_{\psi}^{\psi} \left(\frac{i\pi}{2} - \theta \right) = S_{\psi\psi}^{\psi\psi}(2\theta) R_{\psi}^{\psi} \left(\frac{i\pi}{2} + \theta \right) + S_{\phi\phi}^{\psi\psi}(2\theta) R_{\phi}^{\phi} \left(\frac{i\pi}{2} + \theta \right). \quad (3.14b)$$

Since the Lee–Yang parts satisfy the scalar version of the boundary crossing condition we only have to check that the supersymmetric factors S_{SUSY} and R_{SUSY} satisfy (3.14). Using the integral representations for them this can be proved analytically. We also checked that the matrix parts satisfy the boundary Yang–Baxter equations as well.

It seems plausible that the two supersymmetric reflection factors, $R_0(\theta)R_{\text{SUSY}}(\theta)$ and $R_I(\theta)R_{\text{SUSY}}(\theta)$ are the reflection factors for the two Neveu–Schwarz boundary conditions of the supersymmetric scaling Lee–Yang model, since for the Ramond type boundary conditions we do not expect diagonal reflection factors (the fermion parity can change). It is also natural to think that R_0R_{SUSY} is for the (1,1) boundary condition, because it does not depend on any boundary parameter.

We emphasize that the reflection factors proposed here are different from the non-diagonal one proposed by Ahn and Nepomechie in [12].

3.2 Relation between the boundary parameter b and the boundary coupling h

Following reference [20] it is possible to conjecture the relation between b and the coupling constant of the boundary perturbation, h (a similar argument was used also in [21]). In that paper it was found that the transformation $b \rightarrow 4 - b$ is a symmetry of the model, since this change of b maps the reflection factors of the ground state and excited boundaries into each other. For $b > 2$ the pole at $\theta = \frac{i(b+1)\pi}{6}$ in R_I which corresponds to an excited boundary leaves the physical strip but at the same time the pole at $\theta = \frac{i(5-b)\pi}{6}$ in R_{II} enters. Thus for $b > 2$ R_{II} describes the ground state boundary and R_I the excited boundary. A similar phenomenon is probably to occur in our case, but exactly the same thing can not work, since now the excited boundary state is a doublet while the boundary ground state is a singlet and R_{II} is a 4x4 matrix. However, at the pole R_{II} becomes a 1-dimensional projector. Since the reflection factors are manifestly periodic in b with a period of 12 there is a point ($b = 8$) beyond which the boundary energies swap back and the ground state will be a singlet again. This gives a symmetry $b \rightarrow 10 - b$. Together with the trivial symmetry $b \rightarrow -6 - b$ of the reflection factors this results in a periodicity of the physical spectrum in b with a period of 16. Similarly to the case in [20], the value at half way between the fixed points of the two symmetries should correspond to $h = 0$. This leads to the conjecture for the relation between b and h :

$$h = h_c \sin\left(\frac{(b-1)\pi}{8}\right) \quad (3.15)$$

with $h_c = \alpha m^{3/4}$ where α is some numeric constant and m is some mass scale of the model, e. g. the mass of the particle.

3.3 The massless limit

It is the supersymmetric part R_{SUSY} for which it is easier to calculate the massless limit since it does not contain boundary parameters. All we have to do is to take the limit $\theta \rightarrow \infty$.

$\mathcal{A}_{\pm}(\theta)$ can be written in the following form:

$$\mathcal{A}_{\pm}(\theta) = \sqrt{2} 2^{-\frac{\theta}{i\pi}} \frac{\cos(\frac{\theta}{2i} \mp \frac{\pi}{4})}{\sqrt{\cosh(\theta)}} e^{I(\theta)}, \quad (3.16)$$

where

$$I(\theta) = \int_0^{\infty} \frac{dt}{t} f(t) \sinh\left(\frac{\theta}{i\pi} t\right) = -\frac{1}{2} \int_{-\infty}^{\infty} \frac{dt}{t} e^{it\theta} f(t\pi) \quad (3.17)$$

with

$$f(t) = -\frac{1}{4} \frac{\cosh(\frac{t}{8}) + \cosh^2(\frac{t}{2})}{\cosh^2(\frac{t}{4}) \cosh^2(\frac{t}{2})}. \quad (3.18)$$

Now

$$I(\infty) = -\frac{i\pi}{2} f(0) = \frac{1}{4} i\pi \quad (3.19)$$

so

$$\lim_{\theta \rightarrow \infty} 2^{\frac{\theta}{i\pi}} \mathcal{A}_{\pm}(\theta) = \sqrt{2} \frac{\frac{1}{2} e^{\frac{\theta}{2}} e^{\mp i\frac{\pi}{4}}}{\sqrt{\frac{1}{2} e^{\theta}}} e^{\frac{i\pi}{4}} = e^{\frac{i\pi}{4}(1 \mp 1)}, \quad (3.20)$$

which means that

$$R_{\text{SUSY}}(\theta) \rightarrow \begin{pmatrix} 1 & 0 \\ 0 & i \end{pmatrix}. \quad (3.21)$$

Let us turn to the scalar parts. $R_0(\theta)$ does not depend on the boundary parameters and

$$\lim_{\theta \rightarrow \infty} R_0(\theta) = 1. \quad (3.22)$$

$R_I(\theta)$ does depend on the boundary parameter b . In the massless limit we want to keep h fixed, which means that the sine in (3.15) has to go to infinity in a proper way. This can be achieved only if b becomes complex. We should set $b = -3 - i\hat{b}$, then

$$h = -h_c \cosh\left(\frac{\hat{b}\pi}{8}\right) m^{\frac{3}{4}} \longrightarrow -\frac{h_c}{2} (e^{\frac{\hat{b}\pi}{6}} m)^{\frac{3}{4}}. \quad (3.23)$$

This means that $m e^{\frac{\hat{b}\pi}{6}}$ should be kept fixed while $m \rightarrow 0$ and $\hat{b} \rightarrow \infty$. We also want to keep the physical momentum, $m \cosh(\theta)$ fixed, which implies that $m e^{\theta}$ is constant. We conclude that while $\theta, b \rightarrow \infty$ the combination $\theta - \frac{\hat{b}}{6}\pi$ is fixed. So

$$R_I(\theta) = R_0(\theta) \left(S_{\text{LY}}\left(\theta + \frac{\hat{b}}{6}\pi\right) S_{\text{LY}}\left(\theta - \frac{\hat{b}}{6}\pi\right) \right)^{-1} \longrightarrow S_{\text{LY}}^{-1}\left(\theta - \frac{\hat{b}}{6}\pi\right) = S_{\text{LY}}^{-1}(\hat{\theta} - \theta_{\text{B}}) \quad (3.24)$$

where $\hat{\theta}$ is the pseudo-rapidity and θ_B is related to \hat{b} .¹

We have found that the massless reflection factors for the two NS boundary conditions of the SLY model are

$$\hat{R}_0 = \begin{pmatrix} 1 & 0 \\ 0 & i \end{pmatrix} \quad \text{and} \quad \hat{R}_I(\hat{\theta}) = S_{\text{LY}}^{-1}(\hat{\theta} - \theta_B)\hat{R}_0. \quad (3.25)$$

In the following we will omit the hat in the notation for the pseudo-rapidity.

4 TCSA

The method we use for examining boundary flows is the so-called truncated conformal space approach, or TCSA. In this approach the infinite dimensional Hilbert space is truncated to a finite dimensional vector space by using only those states whose energy is not greater than a threshold value, E_{cut} . This is equivalent to truncating the Hilbert space at a given level. The Hamiltonian is then diagonalised on this truncated space. The original idea was proposed in [22], it was applied for the first time for boundary problems in [20] and in a supersymmetric theory in [23]. The current method is based on the techniques of [24], modified for superconformal minimal models for the first time in [13].

The Hamiltonian of the perturbed superconformal field theory takes the form

$$\hat{H} = \hat{H}_{\text{CFT}} + \hat{H}_{\text{pert}}, \quad (4.1)$$

where \hat{H}_{CFT} is the Hamiltonian of the unperturbed theory

$$\hat{H}_{\text{CFT}} = \hat{H}_{\alpha 0} = \frac{\pi}{R}(L_0 - \frac{c}{24}) \quad (4.2)$$

and \hat{H}_{pert} comes from the perturbation on the strip:

$$\hat{H}_{\text{pert}}^{\text{strip}} = h(\hat{G}_{-1/2}\phi_{1,3})(0,0). \quad (4.3)$$

The location of the left boundary is at $x = 0$ and we are free to choose $t = 0$ for calculating the spectrum. By the exponential map this on the z -plane becomes

$$\hat{H}_{\text{pert}} = h\left(\frac{\pi}{R}\right)^{\Delta_{1,3}+1/2}(\hat{G}_{-1/2}\phi_{1,3})(z=1). \quad (4.4)$$

Thus the complete Hamiltonian on the plane can be written as

$$\hat{H} = \frac{\pi}{R}\left[L_0 - \frac{c}{24} + h\left(\frac{R}{\pi}\right)^{1/2-\Delta_{1,3}}(\hat{G}_{-1/2}\phi_{1,3})(1)\right]. \quad (4.5)$$

¹The method used in [12], taking the joint limits $\theta \rightarrow \infty$, $m \rightarrow 0$ and demanding that the result be finite and unitary, leads to the same result.

Since a numerical calculation requires dimensionless quantities we have to introduce some mass scale, μ and measure the volume (R) and the energies in units of μ . In other words, we use the dimensionless quantities $r = \mu R$, $\varepsilon = E/\mu$, $\kappa = \hbar/\mu^{1/2-\Delta_{1,3}}$ and $\hat{h} = \hat{H}/\mu$:

$$\hat{h} = \frac{\pi}{r} \left[L_0 - \frac{c}{24} + \kappa \left(\frac{r}{\pi} \right)^{1/2-\Delta_{1,3}} (\hat{G}_{-1/2}\phi_{1,3})(1) \right], \quad (4.6)$$

where κ characterizes the relation between the boundary coupling and the chosen mass scale, thus it is not fixed to any preferred value yet.

In order to calculate the eigenvalues of the matrix \hat{h} we choose the basis vectors for the truncated Hilbert space of the form written in (2.4) with $\Delta = \Delta_{1,s}$. After eliminating the null vectors and the corresponding submodules, we obtain a non-orthonormal basis, $\{e_i\}$. Then the matrix elements of the TCSA Hamiltonian are

$$h_{ij} = \frac{\pi}{r} \left[\left(h_i - \frac{c}{24} \right) \delta_{ij} + \kappa \left(\frac{r}{\pi} \right)^{1/2-\Delta_{1,3}} (M^{-1}B)_{ij} \right], \quad (4.7)$$

where M is the inner product matrix

$$M_{ij} = \langle e_i | e_j \rangle, \quad (4.8)$$

and B contains the matrix elements of the perturbing operator:

$$B_{ij} = \langle e_i | (\hat{G}_{-1/2}\phi_{1,3})(1) | e_j \rangle. \quad (4.9)$$

These matrix elements can be calculated using contour integration techniques and the superconformal operator algebra, as worked out in detail in [13].

4.1 TCSA fits

The Bethe–Yang equation for a massless particle moving between the boundaries is

$$e^{ip2R} \hat{R}_0 \hat{R}_I(\theta) = 1, \quad (4.10)$$

that is

$$e^{ip2R} S_{\text{LY}}^{-1}(\theta - \theta_B) \hat{R}_0^2(\theta) = 1. \quad (4.11)$$

Taking the logarithm we get

$$2pR + \delta(\theta - \theta_B) = 2n\pi, \quad (4.12)$$

where

$$\delta(\theta) = \frac{1}{i} \log S_{\text{LY}}^{-1}(\theta), \quad (4.13)$$

and n can be integer or half-integer for the two eigenvalues of \hat{R}_0^2 (1 and -1).

For a massless particle $p = E = \frac{\mu}{2} e^\theta$ where μ is some mass scale. A shift in the pseudo-rapidity θ is equivalent with a change in μ . The shift in θ , $\theta - \theta_B$ can be

compensated by changing μ which for the TCSA means changing the numeric value of the dimensionless coupling κ .

We should note that the Bethe–Yang equations are not derived rigorously for massless particles. However, experience shows that it works and gives the correct energy levels even for rather small volumes. The massless limit of the massive TBA equations are the same as those derived from the massless Bethe–Yang equation and they work in a lot of cases, which is another reassuring fact. We will see that also in our case it gives consistent energy levels.

Equation (4.12) can be solved for r ($pR = ER = \varepsilon r$) for different values of n and we can plot the inverse of the function $r(\varepsilon)$ and compare the lines with the TCSA data, $\varepsilon_{\text{TCSA}}(r)$. For this we have to distinguish the one-particle energy levels. For the multi-particle states we have a coupled system of Bethe–Yang equations that contain also the bulk S-matrix, which makes the behaviour of the energy eigenvalues different for finite volumes. This, in principle, allows us to select the one-particle levels. Furthermore, for large volume (r) the interaction becomes negligible and the asymptotic behaviour of the energies are

$$E_n \sim \frac{\pi}{r}n \quad (4.14)$$

for one-particle states and

$$E_{n_1, n_2, \dots} \sim \frac{\pi}{r} \sum_i n_i \quad (4.15)$$

for multi-particle states. Thus the IR behaviour is the same for one-particle and multi-particle states and for a given (half-)integer number n there is precisely one one-particle state and possibly several multi-particle states with asymptotic energy $n\pi/r$. If for a certain value of n there is only one level, one can be sure that it is a one-particle level. For $n = \frac{1}{2}$ there are no multi-particle states obviously and for greater values of n certain multi-particle states may be forbidden by exclusion rules. For example in the $n = 1$ case the two-particle state corresponding to $1 = \frac{1}{2} + \frac{1}{2}$ is excluded, so for $n = 1/2, 1$ there is only one energy level which corresponds to a one-particle state.

For each value of κ first we must find the appropriate value of θ_B , for example by fitting the lowest energy level which is a one particle level. After this is done, all the other one particle energy eigenvalues should automatically fit the other lines. The result of such a fit can be seen in Figure 1(a) for the NS-NS case with $\kappa > 0$, when only the integer levels of the module (1,3) are in the Hilbert space (see (2.9) and below). As can be seen, the TCSA spectrum possesses the expected features: the lowest energy levels are non-degenerate in the IR and the higher levels are arranged in groups.

In every group there is exactly one level that fits the one-particle Bethe–Yang energy, with integer values n . It is interesting to observe that these levels are always the highest ones in their group, which is due to the fact that the interaction is attractive. The lines of Figure 1(a) not fitted by a solid line correspond to multi-particle states. The number of these levels is neither consistent with bosonic nor

with fermionic exclusion statistics. This suggests that these particles obey some generalised exclusion statistics, similarly to the ordinary Lee–Yang model [25].

One would expect that the other eigenvalue of the reflection factor corresponds to the reflection of the other member of the superdoublet, that is the energy eigenvalues from the half-integer levels (NS- $\widetilde{\text{NS}}$ case) will fit the lines of half-integer values of n . Surprisingly, this is not the case and it is not clear why it does not happen and then what the reflection factor is for these fermionic levels.

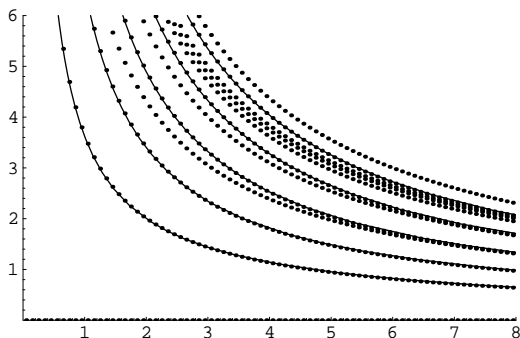
For $\kappa < 0$ ($h < 0$) the spectrum becomes complex, just like for the ordinary Lee–Yang model [20].

Another and more precise approach is obtaining the phase shift $\delta(\theta)$ from the various TCSA eigenvalues and comparing it with the exact function (4.13). From (4.12) one gets

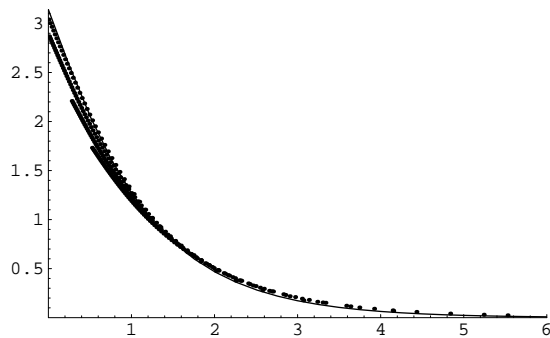
$$\delta_{\text{TCSA}}(\log \frac{E_{\text{TCSA}}}{\mu} - \theta_{\text{B}}) = \delta_{\text{TCSA}}(\log \varepsilon_{\text{TCSA}} - \theta_{\text{B}}) = 2n\pi - 2\varepsilon r, \quad (4.16)$$

It can be seen that our ignorance of the proper mass scale (or the value of θ_{B}) is only a matter of a horizontal shift of the function along the θ -axis while changing the quantum number n shifts the function vertically. In Figure 1(b) the phase shifts calculated from the lowest one particle eigenvalues are plotted onto each other, which shows that the phase shifts extracted from the different one-particle levels are the same. This shows that the massless Bethe–Yang equation is meaningful and gives consistent results. The difference between the phase shifts for small rapidities is due to the truncation errors of the TCSA in the IR.

In Table 1 the phase shift values calculated from the difference of the two lowest TCSA eigenvalues are compared with the theoretical values (4.13). In Figures 1(c) and 1(d) the the TCSA phase shifts obtained from the lowest eigenvalues are plotted together with the proposed phase shift (4.13). As it can be seen there is good agreement.



(a) Energy eigenvalues from the integer levels with the theoretical energies from the reflection factor



(b) $\delta_{\text{TCSA}}(\theta)$ phase shifts calculated from different TCSA eigenvalues

θ_{TCSA}	$\delta(\theta)$	$\delta_{\text{TCSA}}(\theta)$
0.0025	3.1358	3.0401
0.0570	3.0099	2.9276
0.1154	2.8760	2.8076
0.1782	2.7337	2.6796
0.2462	2.5824	2.5426
0.3204	2.4217	2.3961
0.4022	2.2513	2.2391
0.4935	2.0707	2.0707
0.5968	1.8795	1.8898
0.7158	1.6772	1.6953
0.8562	1.4630	1.4860
1.0275	1.2361	1.2606
1.2461	0.9951	1.0179
1.5461	0.7378	0.7567
2.0163	0.4612	0.4765
3.0696	0.1609	0.1765

Table 1: The theoretical phase shift (4.13) and the TCSA result

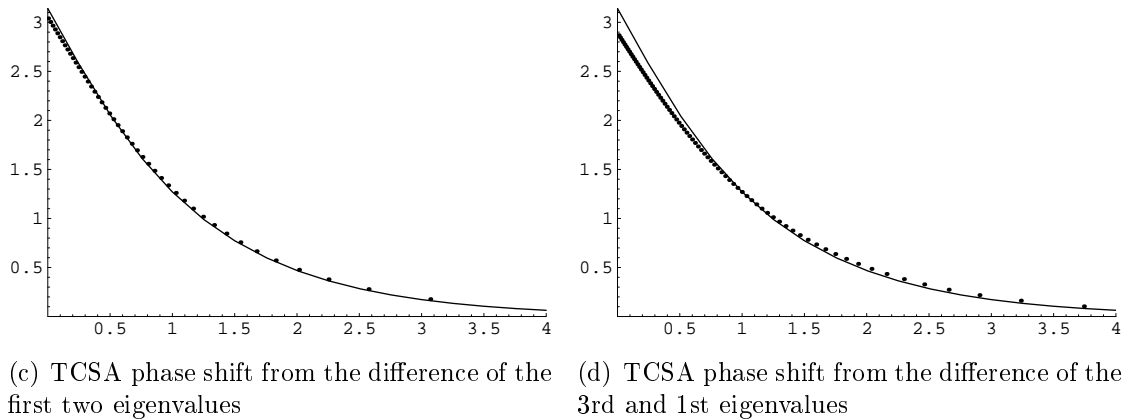


Figure 1: Reflection factor and TCSA spectrum

5 TBA

The Thermodynamical Bethe Ansatz is based on the quantisation of the energy levels using the S-matrices and the reflection factors of the model. The corresponding Bethe–Yang equation takes the following form in terms of the densities for N

particles in the periodic case ([26, 27]):

$$2\pi P(\theta) = m \cosh(\theta) + \int d\theta' \left[\rho(\theta') \Phi_z(\theta - \theta') + \rho_0(\theta') \frac{1}{2} \Phi(\theta - \theta') + \bar{\rho}_0(\theta') \left(-\frac{1}{2}\right) \Phi(\theta - \theta') \right], \quad (5.1)$$

where $\rho(\theta)$ denote the density of the occupied states and $P(\theta)$ the density of available states. Similarly, $\rho_0(\theta)$ denotes the density distribution of real solutions x_j of the equation

$$\prod_{l=1}^N \frac{\tanh\left(\frac{x-\theta_l}{2} - \frac{i\pi}{6}\right)}{\tanh\left(\frac{x-\theta_l}{2} + \frac{i\pi}{6}\right)} = -F, \quad (5.2)$$

(F is the fermion parity) for which $\epsilon_j = +1$ and by $\bar{\rho}_0(\theta)$ the solutions for which $\epsilon_j = -1$.

The kernel functions are

$$\Phi_z(\theta) = \frac{\partial}{\partial \theta} \text{Im} \log \left(\frac{Z(\theta)}{\sinh(\theta)} \right), \quad (5.3a)$$

$$\Phi(\theta) = \frac{\partial}{\partial \theta} \text{Im} \log S_{\text{LY}}(\theta) = -\frac{4\sqrt{3} \cosh(\theta)}{1 + 2 \cosh(2\theta)}, \quad (5.3b)$$

where $Z(\theta)$ is the scalar part of $S_{\text{SLY}}(\theta)$ defined in equation (3.5).

Let us turn to the boundary case. Since the reflection factors are diagonal they do not affect the calculation of the transfer matrix eigenvalues, so in the massless case

$$2\pi P(\theta) = \frac{\mu}{2} e^\theta + \frac{\Psi(\theta)}{2R} + \int d\theta' \left[\rho(\theta') \Phi_z(\theta - \theta') + \rho_0(\theta') \frac{1}{2} \Phi(\theta - \theta') + \bar{\rho}_0(\theta') \left(-\frac{1}{2}\right) \Phi(\theta - \theta') \right], \quad (5.4)$$

where

$$\Psi(\theta) = \frac{\partial}{\partial \theta} \text{Im} \log (\pm \hat{R}_{\text{left}}(\theta - \theta_B) \hat{R}_{\text{right}}(\theta - \theta_B)). \quad (5.5)$$

For $P_0(\theta) = \rho_0(\theta) + \bar{\rho}_0(\theta)$ we have a similar equation, obtained from equation (5.2):

$$2\pi P_0(\theta) = \int d\theta' \rho(\theta') \frac{\partial}{\partial \theta} \text{Im} \log \left(\frac{\tanh\left(\frac{1}{2}(\theta - \theta' - i\frac{\pi}{3})\right)}{\tanh\left(\frac{1}{2}(\theta - \theta' + i\frac{\pi}{3})\right)} \right) = - \int d\theta' \rho(\theta') \Phi(\theta - \theta'). \quad (5.6)$$

Now using the fact that $P_0(\theta) = \rho_0(\theta) + \bar{\rho}_0(\theta)$ and equation (5.6) we can eliminate $\rho_0(\theta)$ from equation (5.4) getting

$$P(\theta) = \frac{\mu}{4\pi} e^\theta + \frac{\Psi(\theta)}{4\pi R} + \left(\rho \star (\Phi_z - \frac{1}{2} \Phi \star \Phi) \right)(\theta) - (\bar{\rho}_0 \star \Phi)(\theta), \quad (5.7)$$

where we introduced the notation

$$(\phi \star \psi)(\theta) = \int \frac{d\theta'}{2\pi} \phi(\theta - \theta') \psi(\theta') \quad (5.8)$$

for the convolution. It turns out that the following identity holds ([12]):

$$(\Phi_z - \frac{1}{2} \Phi \star \Phi)(\theta) = \Phi(\theta). \quad (5.9)$$

The free energy of the system is given by

$$\begin{aligned} f = \int d\theta \left\{ \rho(\theta) \mu e^\theta \right. \\ \left. - T [P(\theta) \log P(\theta) - \rho(\theta) \log \rho(\theta) - (P(\theta) - \rho(\theta)) \log (P(\theta) - \rho(\theta))] \right. \\ \left. - T [P_0(\theta) \log P_0(\theta) - \bar{\rho}_0(\theta) \log \bar{\rho}_0(\theta) - (P_0(\theta) - \bar{\rho}_0(\theta)) \log (P_0(\theta) - \bar{\rho}_0(\theta))] \right\}. \end{aligned} \quad (5.10)$$

Now the densities $\rho(\theta)$, $\bar{\rho}_0(\theta)$ can be varied to minimize the free energy. Using

$$\delta P = \delta \rho \star \Phi - \delta \bar{\rho}_0 \star \Phi, \quad (5.11)$$

$$\delta P_0 = -\delta \rho \star \Phi \quad (5.12)$$

and introducing the quasi-particle energies

$$\frac{\rho(\theta)}{P(\theta)} = \frac{e^{-\epsilon(\theta)}}{1 + e^{-\epsilon(\theta)}}, \quad \frac{\bar{\rho}_0(\theta)}{P_0(\theta)} = \frac{e^{-\epsilon_0(\theta)}}{1 + e^{-\epsilon_0(\theta)}} \quad (5.13)$$

we arrive at the following TBA equations:

$$\epsilon(\theta) = \frac{\mu}{T} e^\theta - (\Phi \star (L - L_0))(\theta), \quad (5.14a)$$

$$\epsilon_0(\theta) = (\Phi \star L)(\theta), \quad (5.14b)$$

where $L(\theta) = \log(1 + e^{-\epsilon(\theta)})$, $L_0(\theta) = \log(1 + e^{-\epsilon_0(\theta)})$.

Now using these equations we can write the extremum of the free energy:

$$\frac{F}{T} = -\frac{1}{2\pi} \int d\theta (\mu e^\theta R + \Psi(\theta)) L(\theta). \quad (5.15)$$

Since the partition function on the cylinder behaves for large R as

$$\log Z_{\alpha\beta} = -\frac{F}{T} \approx \log(g_\alpha g_\beta) - R E_0^{\text{circ}} = \log(g_\alpha g_\beta) - \frac{r}{l} \frac{c_{\text{eff}} \pi}{6} \quad (5.16)$$

we obtain

$$\log(g_\alpha g_\beta) = \frac{1}{2\pi} \int_{-\infty}^{\infty} d\theta \Psi(\theta) \log(1 + e^{-\epsilon(\theta)}). \quad (5.17)$$

This formula is the same given in [28] but it is different from the formula of Ahn and Nepomechie [12] in which $L_0(\theta)$ is used instead of $L(\theta)$. In Figure 2 $\log g_\alpha$ is plotted against $\log \frac{1}{T}$.

In the UV limit $\theta_B \rightarrow -\infty$, the integrand is non-vanishing if $\theta \rightarrow -\infty$ and similarly, in the IR limit $\theta_B \rightarrow \infty$ the non-zero contribution comes from the $\theta \rightarrow \infty$ domain. Using the fact that $\int_{-\infty}^{\infty} d\theta \Phi(\theta) = -2\pi$ we find from the TBA equations (5.14) that

$$L(-\infty) = \log(1 + \sqrt{2}), \quad L(\infty) = 0, \quad (5.18a)$$

$$L_0(-\infty) = \log(2 + \sqrt{2}), \quad L_0(\infty) = \log 2. \quad (5.18b)$$

Now if one of the boundaries has reflection factor \hat{R}_0 and the other one has \hat{R}_I , then from (3.25), (5.3) and (5.5) $\Psi(\theta) = -\Phi(\theta - \theta_B)$, so

$$\log \left(\frac{g_\alpha^{\text{UV}}}{g_\alpha^{\text{IR}}} \right) = \log(1 + \sqrt{2}) = \log \left(\frac{g_{1,3}}{g_{1,1}} \right) \quad (5.19)$$

since the factor $g_\beta = g_{1,1}$ cancels. Thus the TBA predicts the flow $(1, 3) \rightarrow (1, 1)$, which is different from the prediction of [12]. We will see that TCSA supports our result.

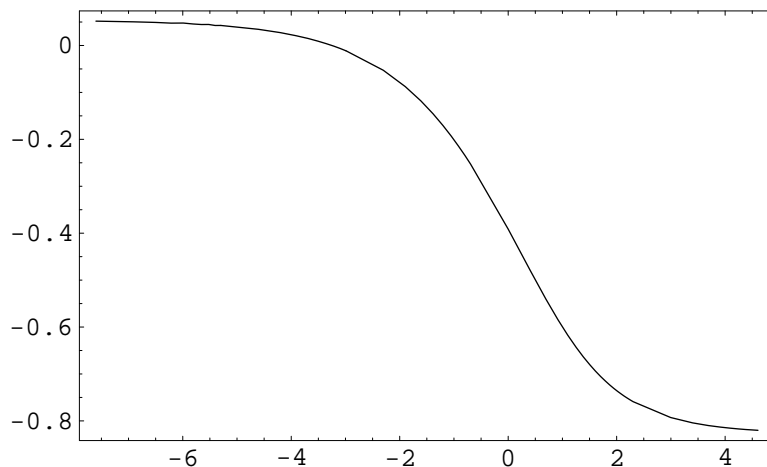


Figure 2: TBA: $\log(g)$ along the flow

6 Flows with TCSA

TCSA can be used to explore the fixed point of the renormalisation group flows. These flows can be implemented by varying the volume r while keeping the coupling constant κ fixed in the Hamiltonian (4.6). Equivalently – and we choose this way – one can keep r fixed and vary κ on some interval. Starting from $\kappa = 0$, which is

the ultraviolet (UV) limit, the matrix \hat{h} can be diagonalised at different values of κ . The flow approaches a fixed point, that is a new supersymmetric conformal boundary condition. We should observe the eigenstates rearranging themselves into some degeneracy pattern from which one can identify the modules (the boundary conditions) using the characters and weight differences of the supersymmetric minimal model.

It is important that the errors of the TCSA diagonalisation cannot be controlled easily. For example, it may happen that before the flow reaches the scaling region the truncation errors start to dominate. If we use various cuts and find that the flow picture does not change drastically (only the precision of the result gets higher with higher cuts), then it means that the unpleasant case mentioned above does not happen.

Of course one can not establish the endpoint of the renormalisation group flow using TCSA. What one can see is that the flow goes in the vicinity of some superconformal boundary condition. The exact infrared fixed point can never be reached by TCSA because of the truncation. We are looking for the range where the TCSA trajectory is closest to the fixed point.

The characters of the (1,3) and (1,1) highest weight representations are

$$\chi_{1,3}(q) = 1 + q^{1/2} + q + q^{3/2} + 2q^2 + 2q^{5/2} + 2q^3 + 3q^{7/2} + 4q^4 + 5q^{9/2} + 5q^5 + 6q^{11/2} + 8q^6 + 9q^{13/2} + 10q^7 + \dots \quad (6.1a)$$

$$\chi_{1,1}(q) = 1 + q^{3/2} + q^2 + q^{5/2} + q^3 + q^{7/2} + 2q^4 + 2q^{9/2} + 2q^5 + 3q^{11/2} + 4q^6 + 4q^{13/2} + 4q^7 + \dots \quad (6.1b)$$

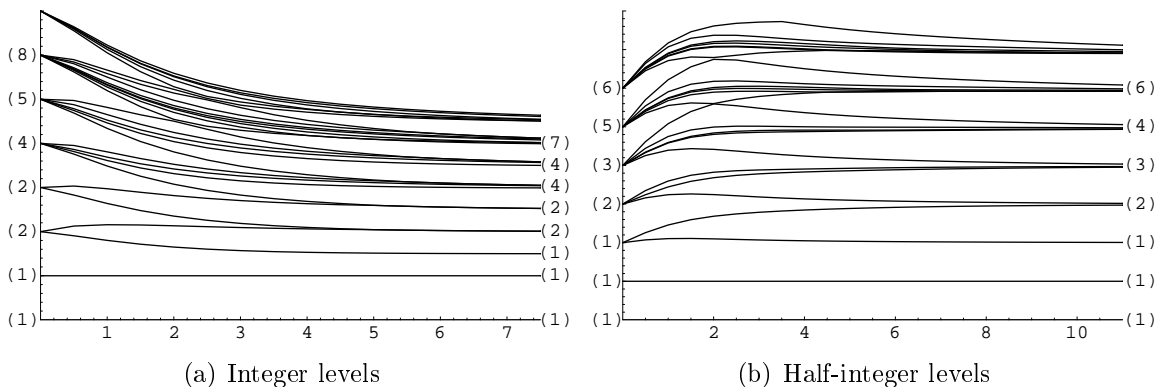


Figure 3: The RG flows starting from the (1,3) NS and $\widetilde{\text{NS}}$ b. c.-s in SM(2,8)

In the TCSA calculations the dimension of the Hilbert space was 393 for the integer levels and 344 for the half-integer ones. In Fig. 3 the normalised energy differences, $(\varepsilon_i - \varepsilon_0)/(\varepsilon_1 - \varepsilon_0)$ are plotted, and the degeneracies are shown in parentheses. We have found that starting with the integer (half-integer) levels of the module (1,3) the flow tends to a degeneracy pattern corresponding to the integer (half-integer)

levels of the module (1,1). Since we did not perturb the (1,1) boundary we can assume that this boundary condition remained the same during the flow. Taking into account that (1,1) is bosonic and (1,3) fermionic, this – keeping in mind the conclusions after equation (2.9) – leads to the conclusion that the flows are

$$(1, 3)_{\text{NS}} \longrightarrow (1, 1)_{\widetilde{\text{NS}}}, \quad (6.2a)$$

$$(1, 3)_{\widetilde{\text{NS}}} \longrightarrow (1, 1)_{\text{NS}} \quad (6.2b)$$

in perfect agreement with the results of the TBA analysis based on our proposed reflection factor.

The flow of the boundary entropy, $\log(g)$ can also be explored numerically using TCSA [14]. The trace in the partition function (2.9) can be approximated by the finite sum over the TCSA eigenvalues. For each value of l one must find the scaling region, the domain in r for which $\log Z$ behaves as in (5.16). The volume r should be great enough for this scaling behaviour, but for too large values the truncation errors start to dominate and spoil this simple linear form. In Figure 4(a) it can be seen that the scaling region is centered around $r/l = 3$ and in Figure 4(b) the logarithm of the partition function is plotted.

The partition function will depend only on the combination $x = hL^{1/2-\Delta_{1,3}} = hL^{3/4} = \kappa l^{3/4}$. After making the linear fit in r/l along the scaling region for different values of x one gets the product of the g -functions as a function of x . However this function generally contains a linear term in L which corresponds to the free energy density coming from the boundaries. In order to get the correct final result this term should be subtracted. We extracted this term numerically from the large L behaviour of the naive fits for the g -function.

The numeric results are compared with the TBA data in Table 2 and they are plotted in Figure 5 together. Unfortunately there is no systematic method for determining the TCSA errors, but one can make estimates for them. One way is comparing the results obtained at different cuts, i. e. at different dimensions of the Hilbert space, here we found that for $x < 1$ the relative error is 0.5–2%. Another source of error is in the choice of the scaling region, the corresponding error is 0.2–0.7%. Finally, the error of the linear fit itself is about 0.2–0.4%. So our estimate for the relative error in the TCSA results is about 1–3% and the TBA and TCSA values for the g -function agree within this error. Apart from the difference due to the truncation errors in g_{TCSA} at large values of x (as in [14]) there is an excellent agreement between the two approaches.

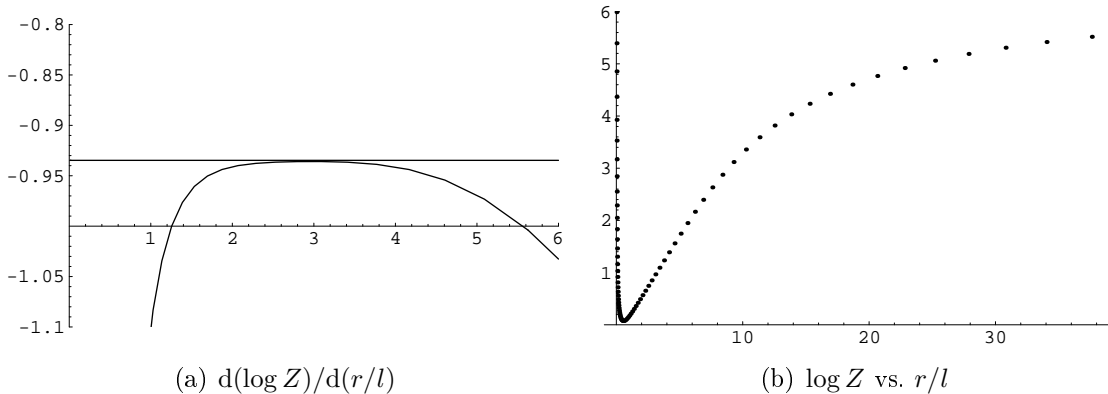


Figure 4: The partition function ($x = 0.1$)

$\log x$	$\log g_{\text{TBA}}$	$\log g_{\text{TCSA}}$
-4.605	-0.0900	-0.0932
-3.912	-0.1013	-0.1059
-3.507	-0.1122	-0.1203
-2.996	-0.1337	-0.1449
-2.302	-0.1846	-0.2008
-1.609	-0.2768	-0.2941
-0.916	-0.4264	-0.4322
-0.693	-0.4864	-0.4906
-0.224	-0.6215	-0.6177
0	-0.6837	-0.6922
0.405	-0.7817	-0.7457
0.693	-0.8347	-0.9015
0.916	-0.8659	-0.9377
1.504	-0.9169	-1.2646

Table 2: TBA and TCSA results for $\log g$

7 Generalisation to $\text{SM}(2, 4n + 4)$

The supersymmetric Lee–Yang model is the first member of the series of superconformal minimal models with $p = 2$, the models $\text{SM}(2, 4n+4)$. Using TCSA we have found that for $\kappa > 0$ starting from the even (odd) levels of any NS module we end up at the even (odd) levels of the (1,1) module (see Figures 6, 7). So the IR fixed point seems to be always the (1,1) boundary condition and depending on the fermion parity of the field corresponding to the UV boundary condition the flow is

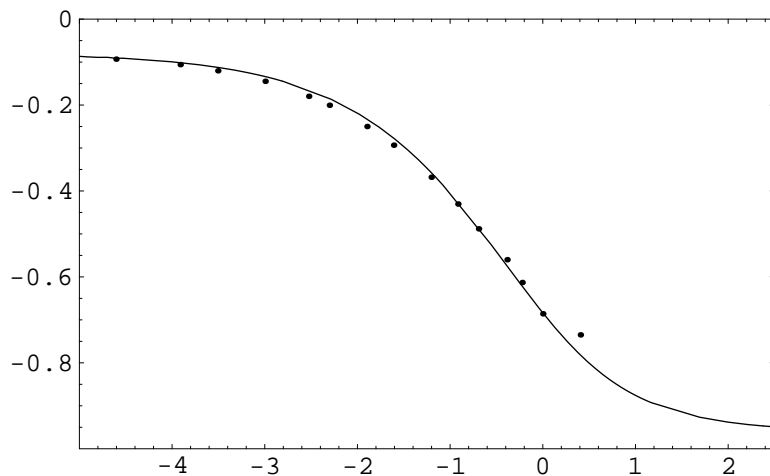


Figure 5: $\log(g)$ vs. $\log(x)$ along the flow, TCSA (dots) and TBA (solid line) results

of type $NS \rightarrow NS$ ($\widetilde{NS} \rightarrow \widetilde{NS}$) or $NS \rightarrow \widetilde{NS}$ ($\widetilde{NS} \rightarrow NS$):

$$(1, 3)_{NS} \longrightarrow (1, 1)_{\widetilde{NS}}, \quad (7.1a)$$

$$(1, 3)_{\widetilde{NS}} \longrightarrow (1, 1)_{NS}, \quad (7.1b)$$

$$(1, 5)_{NS} \longrightarrow (1, 1)_{NS}, \quad (7.2a)$$

$$(1, 5)_{\widetilde{NS}} \longrightarrow (1, 1)_{\widetilde{NS}}, \quad (7.2b)$$

$$(1, 7)_{NS} \longrightarrow (1, 1)_{\widetilde{NS}}, \quad (7.3a)$$

$$(1, 7)_{\widetilde{NS}} \longrightarrow (1, 1)_{NS} \quad (7.3b)$$

\vdots

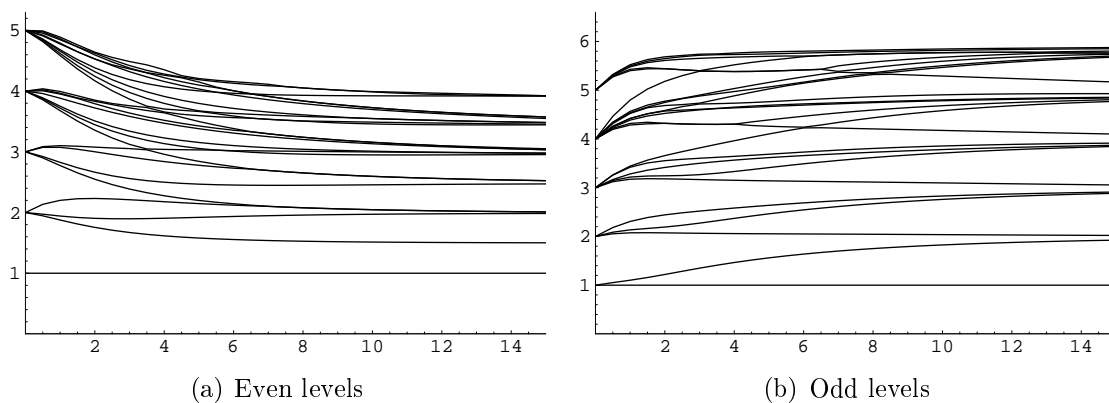


Figure 6: The RG flows starting from b. c. (1,5) in $SM(2,12)$

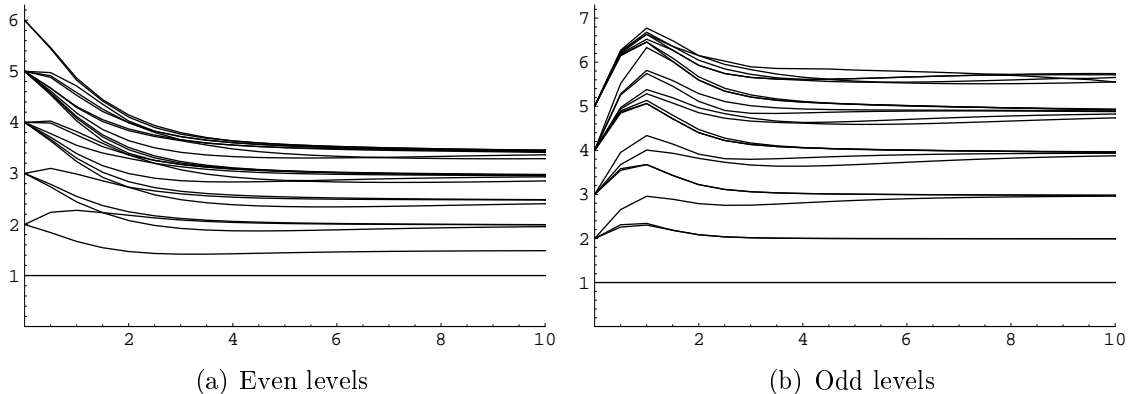


Figure 7: The RG flows starting from b. c. (1,7) in SM(2,16)

8 Conclusions

In this paper we studied the supersymmetric Lee–Yang model (SM(2,8) or M(3,8)) in the presence of boundaries, on a cylinder. First we proposed reflection factors for the NS type boundary conditions by considering our model as a reduction of the supersymmetric sine–Gordon model. The reflection factors of the SSG model contain two boundary parameters but a consistent reduction requires a functional relation between them, leaving only one boundary parameter which is related to the coupling constant of the boundary perturbation of the SLY model. In the massless limit even this boundary parameter gets eliminated.

After determining the massless limit of the reflection factors we compared the energy levels predicted by the Bethe–Yang equation with the numerical spectrum calculated with the Truncated Conformal Space Approach. We have found very good agreement for the even levels of the super Verma module. However, we could not find any reflection factor that could describe the behaviour of the odd energy levels.

Then we turned to the question of the boundary renormalisation group flows of the SLY model. The (1,3) boundary was perturbed by the field $\hat{G}_{-1/2}\phi_{1,3}$ which is a relevant, integrable perturbation that preserves supersymmetry. Using our reflection factor we wrote down the boundary TBA equations and determined the flow of the g -function or equivalently, the boundary entropy. Comparing the UV and IR values of the g -function we concluded that the boundary condition (1,3) flows to the (1,1) boundary condition.

We checked this result using TCSA, diagonalising the Hamilton-operator of the system at various boundary couplings. From the state content and degeneracy pattern of the Hilbert space we could identify the final boundary condition as the boundary condition (1,1), in perfect agreement with the prediction of the TBA analysis. Finally we calculated the g -function along the flow with TCSA, by approximating the partition function and extracting the g -function from the scaling region. The TBA and TCSA results for the change of the boundary entropy along the flow are in excellent agreement.

The proposed reflection factors are different from those of Ahn and Nepomechie [12] but the energy spectrum, the fixed point of the boundary renormalisation group flow and the TBA g -function based on them are in very good agreement with the TCSA results.

At the end of the paper we examined the boundary flows in the generalisations of the SLY model, the superconformal minimal models $SM(2, 4n + 4)$ with TCSA. We found that every Neveu–Schwarz (NS and \widetilde{NS}) boundary condition flows to the (1,1) boundary condition.

Acknowledgement

I would like to thank my supervisor, Gábor Takács for his guidance, help and all the discussions. I am also grateful to Rafael Nepomechie for the useful discussion on the reflection factor.

A The SSG S-matrix

The n th breather in the supersymmetric sine–Gordon model has mass

$$m_n = 2m \sin\left(\frac{n\pi}{2\lambda}\right). \quad (\text{A.1})$$

The SSG breather S-matrix can be written in the form

$$S_{\text{SSG}}^{(i,j)}(\theta) = S_{\text{SG}}^{(i,j)}(\theta) S_{\text{SUSY}}^{(i,j)}(\theta). \quad (\text{A.2})$$

Here [17]

$$S_{\text{SG}}^{(i,j)}(\theta) = \frac{\sinh(\theta) + i \sin\left(\frac{i+j}{2\lambda}\pi\right) \sinh(\theta) + i \sin\left(\frac{i-j}{2\lambda}\pi\right)}{\sinh(\theta) - i \sin\left(\frac{i+j}{2\lambda}\pi\right) \sinh(\theta) - i \sin\left(\frac{i-j}{2\lambda}\pi\right)} \times \prod_{k=1}^{j-1} \frac{\sin^2\left(\frac{i-j-2k}{4\lambda}\pi + i\frac{\theta}{2}\right) \cos^2\left(\frac{i+j-2k}{4\lambda}\pi + i\frac{\theta}{2}\right)}{\sin^2\left(\frac{i-j-2k}{4\lambda}\pi - i\frac{\theta}{2}\right) \cos^2\left(\frac{i+j-2k}{4\lambda}\pi - i\frac{\theta}{2}\right)} \quad (\text{A.3})$$

is the sine–Gordon S-matrix and the supersymmetric factor is

$$S_{\text{SUSY}}^{(i,j)}(\theta) = M^{(i,j)}(\theta) G^{(i,j)}(\theta) \quad (\text{A.4})$$

with

$$M^{(n,m)}(\theta) = \begin{pmatrix} 1 + i \frac{\sin\left(\frac{n\pi}{2\lambda}\right) + \sin\left(\frac{m\pi}{2\lambda}\right)}{\sinh(\theta)} & 0 & 0 & \frac{\sqrt{\sin\left(\frac{n\pi}{2\lambda}\right) \sin\left(\frac{m\pi}{2\lambda}\right)}}{\cosh\left(\frac{\theta}{2}\right)} \\ 0 & 1 - i \frac{\sin\left(\frac{n\pi}{2\lambda}\right) - \sin\left(\frac{m\pi}{2\lambda}\right)}{\sinh(\theta)} & i \frac{\sqrt{\sin\left(\frac{n\pi}{2\lambda}\right) \sin\left(\frac{m\pi}{2\lambda}\right)}}{\sinh\left(\frac{\theta}{2}\right)} & 0 \\ 0 & i \frac{\sqrt{\sin\left(\frac{n\pi}{2\lambda}\right) \sin\left(\frac{m\pi}{2\lambda}\right)}}{\sinh\left(\frac{\theta}{2}\right)} & 1 + i \frac{\sin\left(\frac{n\pi}{2\lambda}\right) - \sin\left(\frac{m\pi}{2\lambda}\right)}{\sinh(\theta)} & 0 \\ \frac{\sqrt{\sin\left(\frac{n\pi}{2\lambda}\right) \sin\left(\frac{m\pi}{2\lambda}\right)}}{\cosh\left(\frac{\theta}{2}\right)} & 0 & 0 & -1 + i \frac{\sin\left(\frac{n\pi}{2\lambda}\right) + \sin\left(\frac{m\pi}{2\lambda}\right)}{\sinh(\theta)} \end{pmatrix} \quad (\text{A.5})$$

and

$$G^{(n,m)}(\theta) = \frac{g(\frac{n+m}{4\lambda})g(\frac{1}{2} - \frac{n-m}{4\lambda})}{g(\frac{1}{2})}, \quad (\text{A.6})$$

$$g(\Delta) = \frac{\sinh(\frac{\theta}{2})}{\sinh(\frac{\theta}{2}) + i \sin(\Delta\pi)} \exp \left\{ \int_0^\infty \frac{dt \sinh(\Delta t) \sinh((1-\Delta)t)}{t \cosh^2(\frac{t}{2}) \cosh(t)} \sinh\left(\frac{it\theta}{\pi}\right) \right\}. \quad (\text{A.7})$$

B SSG reflection factors

The sine-Gordon reflection factor for the n th breather is ([29])

$$R_{\text{SG}}^{(n)}(\theta) = R_0^{(n)}(\theta)R_1^{(n)}(\theta), \quad (\text{B.1})$$

where

$$R_0^{(n)}(\theta) = (-1)^{n+1} \frac{\cos(\frac{\theta}{2i} + \frac{n\pi}{4\lambda}) \cos(\frac{\theta}{2i} - \frac{\pi}{4} - \frac{n\pi}{4\lambda}) \sin(\frac{\theta}{2i} + \frac{\pi}{4})}{\cos(\frac{\theta}{2i} - \frac{n\pi}{4\lambda}) \cos(\frac{\theta}{2i} + \frac{\pi}{4} + \frac{n\pi}{4\lambda}) \sin(\frac{\theta}{2i} - \frac{\pi}{4})} \times \prod_{l=1}^{n-1} \frac{\sin(\frac{\theta}{i} + \frac{l\pi}{2\lambda}) \cos^2(\frac{\theta}{2i} - \frac{\pi}{4} - \frac{l\pi}{4\lambda})}{\sin(\frac{\theta}{i} - \frac{l\pi}{2\lambda}) \cos^2(\frac{\theta}{2i} + \frac{\pi}{4} + \frac{l\pi}{4\lambda})}. \quad (\text{B.2})$$

$R_1^{(n)}(\theta)$, which contains the boundary parameters η and ϑ is different depending on whether n is even or odd:

$$R_1^{(2n)}(\theta) = S^{(2n)}(\eta, \theta)S^{(2n)}(i\vartheta, \theta), \quad (\text{B.3})$$

where

$$S^{(2n)}(x, \theta) = \prod_{l=1}^n \frac{\sin(\frac{\theta}{i}) - \cos(\frac{x}{\lambda} - (l - \frac{1}{2})\frac{\pi}{\lambda})}{\sin(\frac{\theta}{i}) + \cos(\frac{x}{\lambda} - (l - \frac{1}{2})\frac{\pi}{\lambda})} \frac{\sin(\frac{\theta}{i}) - \cos(\frac{x}{\lambda} + (l - \frac{1}{2})\frac{\pi}{\lambda})}{\sin(\frac{\theta}{i}) + \cos(\frac{x}{\lambda} + (l - \frac{1}{2})\frac{\pi}{\lambda})} \quad (\text{B.4})$$

and

$$R_1^{(2n-1)}(\theta) = S^{(2n-1)}(\eta, \theta)S^{(2n-1)}(i\vartheta, \theta) \quad (\text{B.5})$$

with

$$S^{(2n-1)}(x, \theta) = \frac{\cos(\frac{x}{\lambda}) - \sin(\frac{\theta}{i})}{\cos(\frac{x}{\lambda}) + \sin(\frac{\theta}{i})} \prod_{l=1}^{n-1} \frac{\sin(\frac{\theta}{i}) - \cos(\frac{x}{\lambda} - \frac{l\pi}{\lambda})}{\sin(\frac{\theta}{i}) + \cos(\frac{x}{\lambda} - \frac{l\pi}{\lambda})} \frac{\sin(\frac{\theta}{i}) - \cos(\frac{x}{\lambda} + \frac{l\pi}{\lambda})}{\sin(\frac{\theta}{i}) + \cos(\frac{x}{\lambda} + \frac{l\pi}{\lambda})}. \quad (\text{B.6})$$

In the supersymmetric sine-Gordon model the reflection factors are of the form ([8, 6])

$$R_{\text{SSG}}^{(n)}(\theta) = R_{\text{SG}}^{(n)}(\theta) \otimes R_{\text{SUSY}}(\theta). \quad (\text{B.7})$$

In the so-called $BSSG^+$ case, in which the fermion parity is conserved during the reflection

$$R_{\text{SUSY}}(\theta) = \begin{pmatrix} \mathcal{A}_+ & 0 \\ 0 & \mathcal{A}_- \end{pmatrix} \quad (\text{B.8})$$

with

$$\mathcal{A}_{\pm}(\theta) = P\left(\theta + i\frac{\rho}{2}\right)P\left(\theta - i\frac{\rho}{2}\right)\sqrt{2}K(2\theta)2^{-\frac{\theta}{i\pi}}\cos\left(\frac{\theta}{2i} \mp \frac{\pi}{4}\right), \quad (\text{B.9})$$

where for the k th breather $\rho_k = \pi - k\frac{\pi}{\lambda}$. The functions $K(\theta)$, $P(\theta)$ are defined as

$$K(\theta) = \frac{1}{\sqrt{\pi}} \prod_{k=1}^{\infty} \frac{\Gamma(k - \frac{1}{2} + \frac{\theta}{2\pi i})\Gamma(k - \frac{\theta}{2\pi i})}{\Gamma(k + \frac{1}{2} - \frac{\theta}{2\pi i})\Gamma(k + \frac{\theta}{2\pi i})}, \quad (\text{B.10})$$

$$P(\theta) = \prod_{k=1}^{\infty} \frac{\Gamma^2(k - \frac{\theta}{2\pi i})}{\Gamma(k - \frac{1}{4} - \frac{\theta}{2\pi i})\Gamma(k + \frac{1}{4} - \frac{\theta}{2\pi i})} / \{\theta \rightarrow -\theta\}. \quad (\text{B.11})$$

They have the following integral representations:

$$P(\theta) = \exp\left\{-\frac{1}{8}\int_0^{\infty} \frac{dt}{t} \frac{\sinh(\frac{\theta t}{2\pi i})}{\cosh^2(\frac{t}{8})\cosh^2(\frac{t}{4})}\right\}, \quad (\text{B.12})$$

$$K(\theta) = \frac{1}{\sqrt{\cosh(\frac{\theta}{2})}} \exp\left\{-\frac{1}{4}\int_0^{\infty} \frac{dt}{t} \frac{\sinh(\frac{\theta t}{2\pi i})}{\cosh^2(\frac{t}{4})}\right\}. \quad (\text{B.13})$$

Then $R_{\text{SUSY}}(\theta)$ can be written as

$$R_{\text{SUSY}}(\theta) = \frac{\sqrt{2}2^{-\frac{\theta}{i\pi}}}{\sqrt{\cosh(\theta)}} \exp\left\{-\frac{1}{4}\int_0^{\infty} \frac{dt}{t} \frac{\cosh(\frac{\theta t}{2\pi i}) + \cosh^2(\frac{t}{2})}{\cosh^2(\frac{t}{4})\cosh^2(\frac{t}{2})} \sinh\left(\frac{\theta t}{i\pi}\right)\right\} \\ \times \begin{pmatrix} \cos(\frac{\theta}{2i} - \frac{\pi}{4}) & 0 \\ 0 & \cos(\frac{\theta}{2i} + \frac{\pi}{4}) \end{pmatrix}. \quad (\text{B.14})$$

References

- [1] C. Angelantonj, A. Sagnotti: *Open Strings*, *Phys. Rept.* **371** (2002) 1
(hep-th/0204089)
- [2] J. A. Harvey, D. Kutasov, E. J. Martinec: *On the relevance of tachyons*,
(hep-th/0003101)
- [3] H. Saleur: *Lectures on nonperturbative field theory and quantum impurity problems*, (cond-mat/9812110, cond-mat/0007309)

- [4] R. I. Nepomechie: *Consistent superconformal boundary states*, J. Phys. **A34** (2001) 6509 ([hep-th/0102010](#))
- [5] G. Z. Tóth: *$N = 1$ supersymmetric boundary bootstrap*, Nucl. Phys. B **676** (2004) 497 ([hep-th/0308146](#))
- [6] Z. Bajnok, L. Palla and G. Takacs: *Spectrum of boundary states in $N = 1$ SUSY sine-Gordon theory*, Nucl. Phys. **B644** (2002) 509 ([hep-th/0207099](#))
- [7] P. Baseilhac and K. Koizumi: *$N = 2$ boundary supersymmetry in integrable models and perturbed boundary conformal field theory*, Nucl. Phys. **B669** (2003) 417 ([hep-th/0304120](#))
- [8] R. I. Nepomechie: *The boundary supersymmetric sine-Gordon model revisited*, Phys. Lett. **B509** (2001) 183 ([hep-th/0103029](#))
- [9] C. Ahn, R. I. Nepomechie and J. Suzuki: *Finite size effects in the spin-1 XXZ and supersymmetric sine-Gordon models with Dirichlet boundary conditions*, ([hep-th/0611136](#))
- [10] R. I. Nepomechie and C. Ahn: *TBA boundary flows in the tricritical Ising field theory*, Nucl. Phys. **B647** (2002) 433 ([hep-th/0207012](#))
- [11] G. Feverati, P. A. Pearce and F. Ravanini: *Exact $\phi(1,3)$ boundary flows in the tricritical Ising model*, Nucl. Phys. **B675** (2003) 469 ([hep-th/0308075](#))
- [12] C. Ahn and R. I. Nepomechie: *The scaling supersymmetric Yang-Lee model with boundary*, Nucl. Phys. **B594**, (2001) 660 ([hep-th/0009250](#))
- [13] M. Kormos: *Boundary renormalisation group flows of unitary superconformal minimal models*, Nucl. Phys. **B744** (2006) 358 ([hep-th/0512085](#))
- [14] P. Dorey, I. Runkel, R. Tateo and G. Watts: *g -function flow in perturbed boundary conformal field theories*, Nucl. Phys. **B578** (2000) 85 ([hep-th/9909216](#))
- [15] P. Mathieu: *Integrability of perturbed superconformal minimal models*, Nucl. Phys. **B336** (1990) 338
- [16] F. A. Smirnov: *Reductions of the sine-Gordon model as a perturbation of minimal models of conformal field theory*, Nucl. Phys. **B337** (1990) 156
- [17] C. Ahn: *Complete S matrices of supersymmetric Sine-Gordon theory and perturbed superconformal minimal model*, Nucl. Phys. **B354** (1991) 57
- [18] S. R. Coleman and H. J. Thun: *On The Prosaic Origin Of The Double Poles In The Sine-Gordon S Matrix*, Commun. Math. Phys. **61** (1978) 31

- [19] P. Dorey, R. Tateo and G. Watts: *Generalisations of the Coleman–Thun mechanism and boundary reflection factors*, Phys. Lett. **B448** (1999) 249 (hep-th/9810098)
- [20] P. Dorey, A. Pocklington, R. Tateo, G. Watts: *TBA and TCSA with boundaries and excited states*, Nucl. Phys. **B525** (1998) 641 (hep-th/9712197)
- [21] Z. Bajnok, L. Palla, G. Takacs and G. Z. Toth: *The spectrum of boundary states in sine-Gordon model with integrable boundary conditions*, Nucl. Phys. **B622** (2002) 548 (hep-th/0106070)
- [22] V. P. Yurov, Al. B. Zamolodchikov: *Truncated conformal space approach to the scaling Lee-Yang model*, Int. J. Mod. Phys. **A5** (1990) 3221
- [23] Z. Bajnok, C. Dunning, L. Palla, G. Takacs and F. Wagner: *SUSY sine-Gordon theory as a perturbed conformal field theory and finite size effects*, Nucl. Phys. **B679** (2004) 521 (hep-th/0309120)
- [24] H. Kausch, G. Takacs and G. Watts: *On the relation between $\Phi(1,2)$ and $\Phi(1,5)$ perturbed minimal models and unitarity*, Nucl. Phys. **B489** (1997) 557 (hep-th/9605104)
- [25] K. Schoutens: *Exclusion statistics in conformal field theory spectra*, Phys. Rev. Lett. **79** (1997) 2608 (cond-mat/9706166)
- [26] C. r. Ahn: *Thermodynamics and form-factors of supersymmetric integrable field theories*, Nucl. Phys. **B422** (1994) 449 (hep-th/9306146)
- [27] M. Moriconi and K. Schoutens: *Thermodynamic Bethe Ansatz for $N = 1$ Supersymmetric Theories*, Nucl. Phys. **B464** (1996) 472 (hep-th/9511008)
- [28] A. LeClair, G. Mussardo, H. Saleur and S. Skorik: *Boundary energy and boundary states in integrable quantum field theories*, Nucl. Phys. **B453** (1995) 581 (hep-th/9503227)
- [29] S. Ghoshal: *Bound state boundary S matrix of the Sine-Gordon model*, Int. J. Mod. Phys. **A9** (1994) 4801 (hep-th/9310188)